

## Nonclassical rotational behavior at the vicinity of the lambda point

Shun-ichiro Koh

Physics Division, Faculty of Education, Kochi University

Akebono-cho, 2-5-1, Kochi, 780, Japan

(March 21, 2019)

## Abstract

The rotational property of a quantum liquid at the vicinity of the lambda point  $T_\lambda$  is examined. In a liquid helium-4, shear viscosity shows a slight decrease just above  $T_\lambda$ . We suppose that under the strong influence of Bose statistics, the coherent many-body wave function grows to an intermediate size between a macroscopic and a microscopic size just above  $T_\lambda$ , and suppress the shear viscosity. When it is true, it must have a parallel effect on the rotational properties. Beginning with the bosons without the condensate, we make a perturbation calculation of its susceptibility with respect to the repulsive interaction, and examine how, with decreasing temperature, the growth of the coherent wave function gradually changes the rotational behavior of a liquid. It is shown that the moment of inertia slightly decreases just above  $T_\lambda$ , and that the superfluid density in the mechanical phenomena does not always agree with the thermodynamical superfluid density at the vicinity of  $T_\lambda$ . We compare the result with the experiment by Hess and Fairbank.

PACS numbers: 67.40.-w, 67.40.Vs, 67.40.Db, 05.30.Jp

Typeset using REVTeX

---

e-mail address: koh@cc.kochi-u.ac.jp

## I. INTRODUCTION

A natural way to discuss superfluidity in a confined system is to focus on its rotational properties. When a liquid helium-4 is rotated at a temperature far above the point  $T_\lambda$ , it makes a rigid-body rotation with a uniform vorticity  $\text{rot} \mathbf{v} \neq 0$  owing to its viscosity. The angular momentum around z-axis has a form of  $L_z^{\text{cl}} = I_z^{\text{cl}} \omega$ , where  $I_z^{\text{cl}}$  is a classical moment of inertia and  $\omega$  is a rotational velocity of a container. Figure 1 shows the dependence of the angular momentum. When it is cooled to a certain temperature below  $T_\lambda$ , it shows two different behaviors according to the value of  $\omega$ . Below a critical velocity  $\omega_c$ , it abruptly stops rotating just as the system passes the point, and  $\text{rot} \mathbf{v} = 0$  is satisfied over the whole volume of the liquid. On the other hand, under the faster rotation than  $\omega_c$ , the uniform vorticity abruptly concentrates to certain points, forming vortex lines and leaving other areas to satisfy  $\text{rot} \mathbf{v} = 0$ . These phenomena instilled us with the notion that superfluidity abruptly appears at the point.

For the shear viscosity, however, we know a counter example to this notion. In a classical liquid, with decreasing temperature, the shear viscosity gradually increases [1]. In a liquid helium-4, however, it reaches a maximum value at 2.8K, and begins to reduce its value, finally dropping at the point (2.17K). Figure 2 illustrates this temperature dependence [2]. From our viewpoint, it is a remarkable fact that the shear viscosity begins to decrease at  $T_\lambda + 0.6\text{K}$  before the macroscopic condensate appears. The basis of our phenomenological understanding is the two-fluid model, the foundation of which at  $T_\lambda$  has been established by microscopic theories. However, it is questionable that the two-fluid model in a primitive sense is applicable to the explanation of the decrease of shear viscosity above  $T_\lambda$ , because it completely separates the system into the normal and the superfluid part from the beginning, and assumes that the latter abruptly emerges at  $T_\lambda$  [3].

London stressed that superfluidity is not merely the absence of viscosity, but the occurrence of  $\text{rot} \mathbf{v} = 0$ , and proposed an experiment to confirm this point [4], which was later performed by Hess and Fairbank [5]. This means that the complete disappearance of shear

viscosity is attributed to  $\eta = 0$  over the whole volume of a liquid. In the case of the partial decrease of shear viscosity, however, we are led to a different situation. The change of shear viscosity within 0.6 K above  $T_c$  in Fig 2 is exactly this case, and it suggests that under the strong influence of Bose statistics, the coherent many-body wave function just above  $T_c$  grows to a large but not yet macroscopic size. The translational motion of atoms in these coherent wave functions is irrotational, and it should suppress the viscosity just above  $T_c$ .

The existence of irrotational regions in a liquid must have a parallel effect on the rotational properties. It must slightly reduce the moment of inertia  $I_z$  just above  $T_c$ , a possible  $L_z(\omega)$  of which is schematically illustrated by a dotted line d in Fig.1. The rotational properties of a liquid helium-4 has been subjected to considerable experimental and theoretical studies [6]. These studies, however, mainly focus on the dynamics of the quantized vortices in the superfluid phase in situations where the rotational velocity is not so small that the number of vortices are large. After the pioneering work by Hess and Fairbank [5], and by Packard and Sanders [7], the regimes in which only a few vortices are present have rarely been explored. Hence, it is not surprising that almost no precise measurement has been made on  $I_z$  just above the  $T_c$  point.

A similar reason exists in theoretical studies as well. In theories of superfluidity, the infinite-volume limit is often assumed. In  $V \rightarrow \infty$ , the only significant distinction between states is that between the microscopic and the macroscopic one, and therefore there is no room for the intermediate-sized wave functions in the theory. (In  $V \rightarrow \infty$ , "large but not yet macroscopic" is substantially equivalent to "microscopic" [8].) This clear-cut distinction lies behind the two-fluid model, and it leads us to the preoccupied notion that the anomalous mechanical behaviors by superfluidity appear in a mathematically discontinuous manner at the Bose-Einstein condensation temperature  $T_{BEC}$ . (The only exception to this notion is the critical phenomena explained by the idea of universality, which holds only at the critical region  $10^{-1} > T - T_c > 10^{-6}$ .) For the real system, however, the overall transformation occurs more or less continuously, which exhibits its own feature ignored in the concept of universality at a wider temperature region around  $T_c$  than the critical one. For the rotation

of confined system, we cannot ignore the existence of the center of rotation and the boundary of the system, and therefore we must take into account the size of the system. Hence, the validity of the limit  $V \rightarrow \infty$  is worth examination, and the magnitude of phenomena hidden in the  $V \rightarrow \infty$  limit must be estimated by experiments. We think that, although the deviation of the moment of inertia  $I_z$  from its classical value just above  $T_c$  may be small, the essence of superfluidity is revealed in a primitive form in such a regime, which constitutes the necessary condition for discriminating a quantum fluid from a classical fluid.

To consider these problems, we will make a somewhat different approach from conventional ones. At  $T < T_c$ , the existence of the macroscopic coherent wave function  $\psi(r) = \sqrt{n} \exp[iS(r)]$  ( $r$  is a center-of-mass coordinate of many helium-4 atoms) leads to  $\text{rot} \psi = 0$  geometrically, because the condensate momentum  $p$  is expressed by  $p = (\hbar/m) \nabla S$ . Since we will focus on the continuous change of the system around  $T_c$ , we cannot assume from the beginning the sudden emergence of  $\psi(r)$  at  $T_c$ . Rather, considering the Bose system above and below  $T_c$  on a common ground will enable us to study the intricacy underlying the onset of superfluidity. We begin with the Bose system without the condensate, make a perturbation calculation of its susceptibility with respect to the repulsive interaction by taking peculiar graphs reflecting Bose statistics, and examine how the formation of the coherent wave function gradually changes the rotational behavior of the system. As a result, we derive a nonclassical rotational behavior which we normally think comes from  $\text{rot} \psi = 0$ , without assuming  $\text{rot} \psi = 0$  from the beginning. Specifically, we will derive the decrease of  $I_z$  in the rotating repulsive Bose system just above  $T_c$ , and compare it with the data on a liquid helium-4.

This paper is organized as follows. Section 2 recapitulates the definition of the moment of inertia, and explains the physical reason of the nonclassical rotational behavior. Section 3 develops a formalism of the linear response of the system. Using the result in Sec. 3, Sec. 4 re-examines the experiment by Hess and Fairbank, and estimates the size of the intermediate-sized wave function and the strength of repulsive interaction in a liquid helium-4. Section 5 considers the nonlinear response, and Sec. 6 discusses some related problems.

## II. M O M E N T O F I N E R T I A O F T H E R E P U L S I V E B O S E S Y S T E M

### A . M o m e n t o f i n e r t i a

Consider bosons in a uniform rotation around z-axis. For a liquid helium 4, the repulsive particle picture is not so unrealistic as it would be for any other liquid. Hence, as its simplest model, we use

$$H = \sum_p \left( \frac{p^2}{2m} \right) a_p^\dagger a_p + U \sum_{p,p',q} a_{p+p'}^\dagger a_{p'}^\dagger a_p a_q; \quad (U > 0); \quad (1)$$

where  $a_p$  denotes an annihilation operator of a spinless boson.

The hamiltonian in a coordinate system rotating with a container is  $H = H_0 + H_{ex}$ , where  $H_0$  is the total angular momentum. The rotation is equivalent to the application of a probe acting on a sample. The perturbation  $H_{ex} = -\vec{L} \cdot \vec{\omega}$  is cast in the form  $\int d^3r \vec{v}_d(\vec{r}) \cdot \vec{p}$ , in which  $\vec{v}_d(\vec{r})$  serves as the external field. Figure 3 shows a part of the Bose system in a cylindrical container. When the origin of  $\vec{r}$  is put on the center of rotation,  $\vec{v}_d(\vec{r})$  has a concentric-circle structure illustrated by curved arrows in Fig 3. (In the rigid-body rotation,  $\vec{v}_d(\vec{r})$  agrees with the drift velocity at point  $\vec{r}$ .) We define a mass-current density  $\vec{J}(\vec{r})$ , and express the perturbation  $H_{ex}$  as

$$H_{ex} = \int d^3r \vec{v}_d(\vec{r}) \cdot \vec{J}(\vec{r}); \quad (2)$$

Because of  $\text{div} \vec{v}_d(\vec{r}) = 0$ , Eq.(2) says that  $\vec{v}_d(\vec{r})$  acts as a transverse-vector probe to the excitation of bosons. This fact allows us the formal analogy that the response of the system to  $\vec{v}_d(\vec{r})$  is analogous to the response of the charged Bose system to the vector potential  $\vec{A}(\vec{r})$  in the Coulomb gauge [9] [10]. Hence,  $\vec{J}(\vec{r})$  in Eq.(2) has the following form in momentum space being similar to that in the charged Bose system

$$\vec{J}(\vec{q}; \omega) = \sum_{\vec{p}} \left( \vec{p} + \frac{\vec{q}}{2} \right) a_{\vec{p}+\vec{q}}^\dagger a_{\vec{p}} e^{i(\omega - \epsilon_{\vec{p}+\vec{q}} + \epsilon_{\vec{p}})t}; \quad (3)$$

( $\hbar = 1$  and  $m = 1$ ).  $\vec{v}_d(\vec{r})$  is a macroscopic external field causing the spatial inhomogeneity in the container, whereas  $\vec{J}(\vec{r})$  contains both microscopic and macroscopic informations of the system.

As the simplest susceptibility to  $v_d(r)$ , we often use the mass density  $\rho = nm$  ( $n$  is the number density of particles) as  $J(r) = \rho v_d(r)$ . Microscopically, however, one must begin with the generalized susceptibility consisting of the longitudinal and transverse part ( $\chi = \chi_L; \chi_T$ )

$$\chi(q; \omega) = \frac{q \cdot q}{q^2} \chi_L(q; \omega) + \frac{q \cdot q}{q^2} \chi_T(q; \omega) \quad (4)$$

By definition, the mass density  $\rho$  is a longitudinal response to an external force,  $\rho = \chi_L(0; 0)$ . As illustrated in Fig.3, however, the rotational motion of particles is perpendicular to the radial direction, along which the influence of the wall motion extends into the container. Hence, in principle, one must use the transverse susceptibility  $\chi_T(q; \omega)$  for  $v_d(r)$  such as  $J(r) = \lim_{q \rightarrow 0} \frac{1}{q} \chi_T(q; 0) v_d(r)$ .

Using  $\chi = \chi_T(0; 0)$  in the left-hand side of Eq.(2), and using the above  $J(r)$  and  $v_d = r = (y; x; 0)$  in its right-hand side, one obtains the angular momentum  $L_z$  as

$$L_z = \chi_T(0; 0) \int_V (x^2 + y^2) d^3x \quad (5)$$

In a normal fluid, the susceptibility satisfies  $\chi_T(0; 0) = \chi_L(0; 0)$ , and therefore the ordinary use of  $\rho$  is justified. The classical moment of inertia is given by

$$I_z^{cl} = m n \int_V (x^2 + y^2) d^3x \quad (6)$$

In a superfluid, however, the above argument must be altered. For the later use, we define a term proportional to  $q \cdot q$  in  $\chi$  by  $\chi^\wedge$

$$\chi(q; \omega) = \chi_T(q; \omega) + q \cdot q \frac{\chi_L(q; \omega) - \chi_T(q; \omega)}{q^2} \quad (7)$$

where  $\chi^\wedge$  represents the balance between the longitudinal and transverse susceptibility [11]. Using Eqs.(5), (6) and (7), the moment of inertia  $I_z = L_z$  is written as

$$I_z = I_z^{cl} + \lim_{q \rightarrow 0} \frac{1}{q} \frac{q^2}{q \cdot q} \chi^\wedge(q; 0) \quad (8)$$

For the occurrence of nonclassical moment of inertia, the balance between the longitudinal and transverse low-energy excitation must be destroyed. In Eq.(8),  $\lim_{q \rightarrow 0} [(q^2 - q_0^2) \langle \psi(q;0) | \psi(q;0) \rangle]$  corresponds to the superfluid density  $\rho_s$ .

Consider the ideal Bose system. Within the linear response, it is defined as

$$\chi^{(1)}(q; \omega) = \frac{1}{V} \sum_{\mathbf{p}} \langle \exp(i\mathbf{p} \cdot \mathbf{r}) \rangle \langle \psi(\mathbf{q}; \omega) | \psi(\mathbf{q}; 0) \rangle \quad (9)$$

where  $|\psi\rangle$  is the ground state of  $\sum_{\mathbf{p}} \epsilon(\mathbf{p}) \alpha_{\mathbf{p}}^\dagger \alpha_{\mathbf{p}}$ . The term proportional to  $q_0^2$  has a form of

$$\chi^{(1)}(q; \omega) = \frac{q_0^2}{4V} \sum_{\mathbf{p}} \frac{f(\epsilon(\mathbf{p})) - f(\epsilon(\mathbf{p} + \mathbf{q}))}{\epsilon(\mathbf{p}) - \epsilon(\mathbf{p} + \mathbf{q})}; \quad (10)$$

where  $f(\epsilon(\mathbf{p}))$  is the Bose distribution.

(1) If bosons would form the condensate,  $f(\epsilon(\mathbf{p}))$  in Eq.(10) is a macroscopic number for  $p = 0$  and nearly zero for  $p \neq 0$ . Thus, in the sum over  $p$  in the right-hand side of Eq.(10), only two terms corresponding to  $p = 0$  and  $p = -q$  remain, with a result that

$$\chi^{(1)}(q; 0) = \rho_s(T) \frac{q_0^2}{q^2}; \quad (11)$$

where  $\rho_s(T) = m n_c(T)$  is the thermodynamical superfluid density, and  $n_c(T)$  is the number density of particles participating in the condensate. Equation.(8) with Eq.(11) leads to

$$I_z = I_z^{cl} - 1 - \frac{\rho_s(T)}{q^2}; \quad (12)$$

(2) When bosons form no condensate, the sum over  $p$  in Eq.(10) is carried out by replacing it with an integral, and one notices that  $q^2$  dependence disappears in the result. Hence, using such a  $\chi^{(1)}(q; \omega)$  in Eq.(8) leads to  $I_z = I_z^{cl}$  at  $q \rightarrow 0$ . This means that, without the interaction between particles, BEC is the necessary condition of the nonclassical moment of inertia.

Under the repulsive interaction, however, the above argument is seriously affected. To see this, we must begin with a physical argument.

We have a physical reason to expect the decrease of the moment of inertia in bosons at low temperature. The relationship between the low-energy excitations and Bose statistics dates back to Feynman's argument on the scarcity of the excitation in a liquid helium [12], in which he explained how Bose statistics affects the many-body wave function in configuration space. To the rotating bosons, we will apply his explanation.

(1) In Fig.3 (a), a liquid (white circles) is in the BEC phase, and the wave function has permutation symmetry everywhere in the container. Assume that the rotation of a container (depicted by curved arrows) moves white circles on a solid-line radius to black circles on a one-point-dotted-line radius (a transverse excitation). At first sight, these displacements seem to be a large-scale configuration change, but this result is reproduced by a set of slight displacements (depicted by short thick arrows) from positions in the initial configuration to black circles after rotation. For any particle after rotation, it is possible to find a particle being close to it in the initial configuration. In Bose statistics, owing to permutation symmetry, one cannot distinguish between two types of particles after rotation, one moved from the neighboring position by the short arrow, and the other moved from distant initial positions by the long arrow. Even if the displacement made by the long arrows is a large displacement in classical statistics, it is only a slight displacement by the short arrows in Bose statistics.

Let us imagine this situation in the  $3N$ -dimensional configuration space. The above feature of Bose statistics means that in the configuration space, the excited state driven by rotation lies close to the ground state. Since the excited state is orthogonal to the ground state, the wave function corresponding to the excited state must spatially oscillate. Accordingly, the many-body wave function of the transversely excited state oscillates within a small distance in configuration space. Since the kinetic energy of the system is determined by the  $3N$ -dimensional gradient of the wave function, this steep rise and fall of the amplitude means that the energy of the transverse excitation is not small even at  $q = 0$ , leading to the



scarcity of the low-energy transverse excitation. This is the reason of  $\epsilon^T(q;0) \neq 0$  at  $q \neq 0$  below  $T_c$ , whereas the particle conservation asserts that  $\epsilon^L(q;0) = 0$  is valid both above and below  $T_c$ . Hence,  $\epsilon^T(q;0)$  in Eq.(7) changes to  $\epsilon^L(q;0) = 0$  at  $q \neq 0$ , leading to  $I_z = 0$  in Eq.(8). (This mechanism underlies the geometrical condition  $\text{rot} v_s = 0$ .)

(2) At high temperature, the coherent wave function has a microscopic size. If a long arrow of  $v_d(r)$  takes a particle to a position beyond the coherent wave function including that particle, one cannot regard the particle after rotation as an equivalent of the initial one. The mechanism below  $T_c$  does not work for the large displacement extending over two different wave functions. Hence, we obtain  $\epsilon^T(q;0) = \epsilon^L(q;0)$  at  $q \neq 0$ , and  $I_z = I_z^{\text{cl}}$ .

(3) Figure 3(b) shows the boson system at the vicinity of  $T_c$  in the normal phase, in which the coherent many-body wave function grows to a large but not yet a macroscopic size (regions enclosed by a dotted line). The permutation symmetry holds only within each of these regions. When particles are moved from a region A to another region A', the mechanism below  $T_c$  does not work.

(a) The repulsive interaction  $U$  between particles, however, affects this situation. In general, when one moves a particle in the interacting system, it induces the motions of other particles. In particular, the large-distance displacement of a particle in coordinate space causes the excitation of many particles, and therefore it needs a large excitation energy. This means that in the low-energy excitation of the system, one observes mainly the short-distance displacement of particles. When applying this tendency to the low-energy excitation of repulsive bosons, one knows that excited particles are not likely to go beyond a single coherent wave function, but likely to remain in it, and therefore the mechanism working below  $T_c$  works just above  $T_c$  as well. This view will be tested as follows. If we increase the strength of  $U$  in  $\epsilon^L(q;0)$ , the excited bosons get to remain in the same coherent wave function, and therefore the low-energy transverse excitation will raise its energy owing to Bose statistics as discussed in (1). Hence, the condition of  $\epsilon^L(q;0) = \epsilon^T(q;0)$  at  $q \neq 0$  will be violated at a certain critical value of  $U$ . Alternatively, if we decrease the temperature at a given  $U$ , the above condition will be violated at a certain temperature  $T_{\text{on}}$ .

(b) A geometric feature inherent in the rotation will play an important role in the above mechanism. The external field  $v_d(r)$  has the structure of concentric circle, hence the center of rotation is a fixed point. The displacements of particles near the center is so small that they do not go beyond a single coherent wave function (a region B in Fig.3(b)). The center of rotation is the most probable point for the mechanism discussed in (a) to work. Hence, the region near the center is most likely to decouple from the motion of container. With decreasing temperature, this decoupling will extend from the center to the wall, which depends on the rotational velocity.

To formulate these mechanisms, we consider the perturbation expansion of  $\chi$  with respect to  $U$  in Sec.3. After comparing it with the experiment in Sec.4, we extend it to the nonlinear response to  $v_d(r)$  in Sec.5.

### III. LINEAR RESPONSE

We will formulate the moment of inertia in the repulsive Bose system at the vicinity of  $T_c$ . In the integrand of Eq.(9), one must use, instead of  $|\psi\rangle$ , the ground state  $|\psi_g\rangle$  of Eq.(1) as follows

$$\langle G | \hat{T} \hat{J}(\mathbf{x}; \mathbf{p}) \hat{J}(0;0) | \psi_g \rangle = \frac{\langle 0 | \hat{T} \hat{J}(\mathbf{x}; \mathbf{p}) \hat{J}(0;0) \exp \left( -\frac{\hbar}{R} \int_0^1 d\tau \hat{H}_I(\tau) \right) | \psi_g \rangle}{\langle 0 | \exp \left( -\frac{\hbar}{R} \int_0^1 d\tau \hat{H}_I(\tau) \right) | \psi_g \rangle}; \quad (13)$$

where  $\hat{H}_I(\tau)$  represents the repulsive interaction. Figure 4 illustrates the current-current response tensor  $\hat{J}(\mathbf{x}; \mathbf{p}) \hat{J}(0;0)$  (a lower bubble in Fig.4(a)) in the medium: Owing to  $\exp(-\frac{\hbar}{R} \int_0^1 d\tau \hat{H}_I(\tau))$  in Eq.(13), scatterings of particles frequently occur in  $|\psi_g\rangle$  as illustrated by an upper bubble with a dotted line  $U$  in Fig.4(a). (The black and white circle represents a coupling to  $v_d(q)$  and to  $U$ , respectively.) The state  $|\psi_g\rangle$  includes many bubbles with various momentums. A solid line with an arrow represents

$$G(i!_n; p) = \frac{1}{i!_n (p) + \mu}: \quad (14)$$

( $\mu$  is a chemical potential implicitly determined by  $V^{-1} [\exp(\beta(\mu + \epsilon)) - 1]^{-1} = n$ ).

Owing to the repulsive interaction, the boson has a self energy  $\epsilon > 0$  (we ignore its !

and  $p$  dependence by assuming it small). With decreasing temperature, the negative at high temperature approaches a small positive value of  $\chi$ , finally reaching Bose-Einstein condensation satisfying  $\chi = 0$ .

When the system is just above  $T_c$  in the normal phase, particles in the ground state  $|0\rangle$  are under the strong influence of Bose statistics. Hence, the perturbation must be developed in such a way that, as the order of the perturbation increases, the susceptibility gradually includes a new effect owing to Bose statistics. Specifically, the lower bubble  $\hat{J}^-(x; 0)$  and the upper bubble in Fig.4 (a) form a coherent wave function as a whole. When one of the two particles in the lower bubble and in the upper bubble have the same momentum ( $p = p^0$ ), and the other in both bubbles have another same momentum ( $p + q = p^0 + q^0$ ) in Fig.4 (a), a graph made by exchanging these particles must be included in the expansion. Such a transformation in Fig.4 (a) takes place as follows. The exchange of two particles having  $p$  and  $p^0 (= p)$  by thick white arrows yields Fig.4 (b). Further, the interchange of two particles having  $p + q$  and  $p + q^0 (= p + q)$  in Fig.4 (b) by thick white arrows yields Fig.4 (c). The result is that two bubbles with the same momentum are linked by the repulsive interaction, whose contribution to  $\chi$  is given by

$$U \frac{1}{V} \sum_p \left( p + \frac{q}{2} \right) \left( p + \frac{q}{2} \right) \left[ \frac{f(p + \frac{q}{2})}{1 + f(p)} \frac{f(p + q + \frac{q}{2})}{f(p + q)} \right]^2 : \quad (15)$$

(a) With decreasing temperature, the coherent wave function grows to a large size, and the interchange of particles owing to Bose statistics like Fig.4 occurs many times. Hence, one cannot ignore the higher-order terms in Eq.(13), which become more significant with the growth of the coherent wave function.

(b) Among many particles contributing to Eq.(15), particles stationary to a container play a dominant role. Specifically, a term with  $p = 0$  in Eq.(15) corresponds to an excitation from the rest particle, and that with  $p = -q$  corresponds to a decay into the rest one.

These considerations (a) and (b) lead to the following form of  $\chi^{(1)}(q; 0)$  at the vicinity of  $T_c$

$$\chi^{(1)}(q;0) = \frac{q}{2} \frac{q}{V} \frac{1}{\sum_{l=0}^{\infty} U^l F(q)^{l+1}}; \quad (16)$$

where

$$F(q) = \frac{(\exp(-\frac{q^2}{2m}))^{1/2} (\exp(-\frac{q^2}{2m} + \frac{q^2}{2m}))^{1/2}}{(q)}; \quad (17)$$

is a positive monotonously decreasing function of  $q^2$ , which approaches zero as  $q^2 \rightarrow \infty$ .

At a high temperature ( $T \rightarrow 0$ ) in which  $F(q)$  is small, a small  $F(q)$  guarantees the convergence of an infinite series in  $\chi^{(1)}(q;0)$  of Eq.(16), with a result that

$$\chi^{(1)}(q;0) = \frac{q}{2} \frac{q}{V} \frac{1}{1 - U F(q)}; \quad (18)$$

With decreasing temperature, however, the negative  $U$  gradually approaches 0, hence

$U \rightarrow 0$ . Since  $F(q)$  increases as  $U \rightarrow 0$ , it makes the higher-order term significant in Eq.(16). An expansion form of  $F(q) = F(0) + a_2 q^2 + \dots$  around  $q=0$  has a form such as

$$F(q) = \frac{1}{4 \sinh^2 \frac{j [T]}{2}} + \frac{1}{2} \frac{1}{\tanh \frac{j [T]}{2}} \frac{q^2}{2m} + \dots; \quad (19)$$

At  $q \rightarrow 0$ , the denominator  $1 - U F(q)$  in the right-hand side of Eq.(18) has a form of  $[1 - U F(0)] + U a_2 q^2$ . In  $U \rightarrow 0$ ,  $U F(0)$  increases and finally reaches 1, that is,

$$U = 4 \sinh^2 \frac{j [T]}{2} \frac{[U]}{2}; \quad (20)$$

At this point, the denominator in the right-hand side of Eq.(18) gets to begin with  $q^2$ , and  $\chi^{(1)}(q;0)$  therefore changes to a form of  $q/q = q^2$  at  $q \rightarrow 0$ . This means that a non-zero coefficient  $F(0) = (2V U a)$  of  $q/q = q^2$  appearing in Eq.(18) gives a non-zero value of  $\chi^{(1)}(q;0) \propto T(q;0)$  in Eq.(7), hence the moment of inertia shows the nonclassical behavior in Eq.(8). From now, we call  $T$  satisfying Eq.(20) the onset temperature of the nonclassical moment of inertia  $T_{on}$  [13].

At the vicinity of  $T$ , Eq.(20) is approximated as  $U = -2 [T - (U)]^2$  for a small  $U$ . This condition has two solutions  $T = (U) \pm \sqrt{U/k_B T}$ . It is generally assumed

that the repulsive Bose system undergoes BEC as well as a free Bose gas. Hence, with decreasing temperature,  $\langle T \rangle$  in the presence of repulsive interaction  $U$  should reach  $\langle U \rangle$  at a finite temperature, during which course the system necessarily passes a state satisfying  $\langle T \rangle = \langle U \rangle = \frac{p}{U k_B T}$  [14]. One concludes that the nonclassical rotational behavior always occurs prior to BEC in the repulsive bosons, that is,  $T_{on} > T^*$ .

The chemical potential  $\mu$ , hence  $\beta\mu$  as well, determines the size of the coherent many-body wave function [15] [16], which corresponds to the size of regions enclosed by a dotted line in Fig.3 (b). The emergence of  $q^{-2}$  singularity in  $\hat{\chi}^{(1)}(q;0)$  in the process of  $\beta\mu \rightarrow 0$  is a mathematical expression of the instability mechanism induced by the growth of the coherent wave function. When  $U$  is small, this instability occurs after the wave function grows to a large size corresponding to a small  $\beta\mu$ . When  $U$  is large, this instability already occurs at a larger  $\beta\mu$  in which the wave function is smaller than the former one.

At the onset temperature  $T_{on}$ , substituting Eq.(19) into Eq.(18), we find  $\hat{\chi}^{(1)}$  at  $q \rightarrow 0$

$$\hat{\chi}^{(1)}(q;0) = \frac{2m}{U_{on}} \frac{1}{V} \tanh \left[ \frac{j_{on}(T_{on})}{2} \right] \frac{q}{q^2}; \quad (21)$$

and with the aid of Eq.(20)

$$\hat{\chi}^{(1)}(q;0) = \frac{1}{V} \frac{m}{\sinh j_{on}(T_{on})} \frac{q}{q^2}; \quad (22)$$

$\hat{\chi}^{(1)}(q;0)$  is given by

$$\hat{\chi}^{(1)}(q;0) = m c(T_{on}) n_0(T_{on}) \frac{q}{q^2}; \quad (23)$$

where

$$n_0(T) = \frac{1}{V} \frac{1}{\exp(j(T)) - 1}; \quad (24)$$

is the number density of  $p=0$  bosons, and

$$c(T) = \frac{2}{\exp(j(T)) + 1} \quad (25)$$

is a Fermi-distribution-like coefficient. For the finite system just above  $T^*$ ,  $n_0(T)$  has a large but not yet macroscopic value. In the theoretical limit  $V \rightarrow \infty$ , this quantity is normally

regarded to be zero. In real finite system, however, its magnitude must be estimated by experiments (see Sec.4). Using Eq.(23) in Eq.(8), we obtain

$$I_z(T_{on}) = I_z^{cl} - 1 - c(T_{on}) \frac{n_0(T_{on})}{n} \quad I_z^{cl} - 1 - \frac{\hat{s}_s(T_{on})}{n} : \quad (26)$$

where  $\hat{s}_s(T) = m c(T) n_0(T)$  is the mechanical superfluid density.

$\hat{s}_s(T)$  reflects the intermediate-sized coherent wave function. "Intermediate" means that it does not play the role of order parameter characterizing the thermodynamical phase, but it affects mechanical properties of the system. At  $T = T_{on}$ , the system shows a small but finite jump from  $I_z^{cl}$  to  $I_z$ , which is proportional to  $n_0(T_{on})$ . Since  $c(T_{on})$  has an order of one, the magnitude of this jump is determined mainly by the non-macroscopic  $n_0(T_{on})$ , and the moment of inertia therefore only slightly decreases from the classical value. (This does not mean that the thermodynamical quantities show a finite jump.) At  $T < T_{on}$ , the moment of inertia varies with  $T$  following  $I_z(T)$  in Eq.(26). Equation (26) determines an initial slope of the dotted curve  $d$  at  $\phi = 0$  in Fig.1. When the system reaches  $T = T_c$ , the condition of  $\phi = 0$  makes  $\hat{s}_s(T) = \hat{s}_s(T)$  because of  $c(T) = 1$ ,  $n_0(T) = n_c$ , which shows a natural connection of Eq.(26) to Eq.(12) with the thermodynamical  $\hat{s}_s(T)$ . While the thermodynamical  $\hat{s}_s(T)$  satisfy  $\hat{s}_s = (m^2 k_B T / \hbar^2) j^2$  at  $T < T_c$ , one can expect no simple relation of the mechanical  $\hat{s}_s(T)$  with the thermodynamical quantities at  $T < T < T_{on}$ .

#### IV. COMPARISON WITH EXPERIMENTS

##### A. The experiment by Hess and Fairbank revisited

Hess and Fairbank, after they confirmed that a superfluid  $^4$ He remained at rest under the extremely slow rotation, made another type of experiment in their classic paper Ref. [5]. First, at an initial temperature  $T_1$  below or above  $T_c$ , they rotated a liquid helium  $^4$ , contained in a small cylinder of radius  $R = 0.44$  mm, at  $\omega = 1.13$  rad/s. Later they heated it up to the temperature as it comes into rigid-body rotation, and precisely measured a small change of the angular velocity. Using Eq.(12), the rotational energy before

heating is  $I_z = I_z^{\text{cl}}(1 - \rho_s)$ , whereas it changes to  $I_z = I_z^{\text{cl}}(\rho_s)$  after heating. By the conservation of energy, the former must be equal to the latter, with a result that  $\rho_s = \rho_s$ . Below  $T_\lambda$ , a fraction of liquid does not participate in the rotation, whereas after heating it does. The rotation after heating therefore always becomes slower, and  $\rho_s = \rho_s$  is positive. They plotted  $\rho_s$  as a function of initial temperature  $T_1$  (Fig 2 of Ref. [5]).

When the initial temperature  $T_1$  was lower than  $T_\lambda$ ,  $\rho_s$  was properly explained by the theoretical value of  $\rho_s(T_1) = \rho_s$ . If the two-fluid model is exactly valid near  $T_\lambda$ ,  $\rho_s$  must vanish at  $T > T_\lambda$ . Hence,  $\rho_s$  measured under the condition of  $T_1 > T_\lambda$  must be exactly zero. For  $T_1 = T_\lambda + 0.03\text{K}$  and  $T_\lambda + 0.28\text{K}$ , however, the measured  $\rho_s$  in Ref [5] were not exactly zero. Although the error bars were large compared with its absolute values, its central values were significantly different from zero:  $\rho_s = 4 \times 10^{-5}$  at  $T_1 = T_\lambda + 0.03\text{K}$ , and  $1.5 \times 10^{-5}$  at  $T_\lambda + 0.28\text{K}$ . A natural interpretation of this result is that these  $T_1$ 's were lower than the onset temperature  $T_{\text{on}}$  of the nonclassical moment of inertia, and at such  $T_1$ 's,  $I_z$  was already slightly smaller than its classical value. If it is true, instead of Eq.(12),  $I_z(T) = I_z^{\text{cl}}(1 - \rho_s(T))$  (Eq.(26)) must be used, and we obtain  $\rho_s = \rho_s(T_1)$ . Hence, we obtain  $\rho_s(T_\lambda + 0.03\text{K}) = 8 \times 10^{-5}$ , and  $\rho_s(T_\lambda + 0.28\text{K}) = 3 \times 10^{-5}$ . Since the number density of atoms in a liquid helium 4 is  $n = 2.2 \times 10^{22} \text{ atom/cm}^3$ , we have  $n_0 = 10^{18} \text{ atom/cm}^3$ . This is an experimental estimation of the number of helium 4 atoms participating in the intermediate-sized coherent wave function in a bulk helium 4 just above  $T_\lambda$ . Two temperatures,  $T_\lambda + 0.03\text{K}$  and  $T_\lambda + 0.28\text{K}$ , are situated within the temperature region ( $T_\lambda < T < 2.8\text{K}$ ) in which the viscosity begins to decrease above  $T_\lambda$  in Fig 2. In Ref. [5], the author's focus was on the rigidity of a superfluid against the rotation (the result was later named Hess-Fairbank effect), and they did not mention the small non-zero value of  $\rho_s$  above  $T_\lambda$ . Although this point did not attract the interest of many people, it is worth studying closely in future.

## B. An estimation of the repulsive interaction $U$

Let us make an estimation of the repulsive interaction  $U$  using Eq.(20), thus using  $U_{\text{on}} = \frac{2}{\text{on}} (\dots)^2$ . (1) For the present, we suppose  $T_{\text{on}} = 2.8\text{K}$  by assuming that the decrease of viscosity in Fig.2 directly reflects the emergence of the intermediate-sized coherent wave function. (2) We assume that  $\chi(T)$  ( $U$ ) in Eq.(20) follows the formula

$$\chi(T) \quad (U) = \frac{g_{3=2}(1)}{2^{\frac{1}{2}}} \frac{1}{k_B T} \left( \frac{T}{T_0} \right)^{3=2} \frac{1}{1} ; \quad (27)$$

( $g_a(x) = \frac{1}{n} x^n = n^a$ ) on the assumption that the particle interaction  $U$  and the particle density of a liquid helium-4 are renormalized to  $T = 2.17\text{K}$  (an approximation that dates back to London). Hence, we obtain a rough estimation of  $U$  as  $0.5 \times 10^{17}$  erg. This value is approximately close to the repulsive interaction  $U_c$  obtained by Bogoliubov's spectrum  $c = \frac{1}{(h=m)} \frac{1}{4} \frac{1}{na}$ , but somewhat smaller than it. (The velocity of sound  $c = 220 \text{ m/s}$  of a liquid helium-4 near  $T$  gives a scattering length  $a = 0.7 \text{ nm}$ , hence  $U_c = \hbar^2/(ma^2) = 3.4 \times 10^{17}$  erg.) It is a difficult problem to relate these values to the realistic potential between helium-4 atoms such as the Lennard-Jones potential  $U(r) = 4 \left[ \left( \frac{2.556}{r} \right)^{12} - \left( \frac{2.556}{r} \right)^6 \right]$  with  $U = 1.41 \times 10^{15}$  erg.

## V. NONLINEAR RESPONSE

When the precise measurement of  $I_z$  is performed, the dynamic response of  $I_z(\omega)$  will become a next subject, which appears in the nonlinear response of the system. As discussed in Sec.2,  $J$  contains both microscopic and macroscopic informations, whereas  $v_d(r)$  is a macroscopic external field, and therefore the susceptibility connecting  $J$  and  $v_d$  appears as  $J(r) = \lim_{q \rightarrow 0} \frac{1}{h} \frac{1}{i} \chi(q;0) v_d(r)$ . Hence, we do not consider a general form of the nonlinear susceptibility, but a correction term to the linear response, such as  $J = [\chi^{(1)} + \chi^{\text{non}}(v_d)] v_d$ . Since  $\chi^{\text{non}}(v_d)$  does not depend on the direction of  $v_d$ ,  $\chi^{\text{non}}(v_d)$  must include even powers of  $v_d$ .



For this phenomenon, we define some quantities. The current  $J(r) = \mathbf{T}(0;0)\mathbf{v}_d(r)$  in Sec.2.A is replaced by  $J(r) = \mathbf{T}(0;0;\mathbf{r})\mathbf{v}_d(r)$ , where  $r = \sqrt{x^2 + y^2}$  is a distance from the center of rotation. Correspondingly, instead of Eq.(5) and (8), we define

$$L_z = \frac{1}{V} \int_V \mathbf{T}(0;0;\mathbf{r}) r^2 d^3\mathbf{x} \quad ; \quad (28)$$

and

$$I_z(\omega) = I_z^{cl} \lim_{q \rightarrow 0} \frac{1}{q} \int_V \frac{q^2}{q} \hat{\mathbf{T}}(q;0;\mathbf{r}) r^2 d^3\mathbf{x} \quad ; \quad (29)$$

The position-dependent rotational velocity is defined as

$$\omega(r) = \frac{1}{V} \lim_{q \rightarrow 0} \frac{1}{q} \int_V \frac{q^2}{q} \hat{\mathbf{T}}(q;0;\mathbf{r}) r^2 d^3\mathbf{x} \quad ; \quad (30)$$

We extend the mechanical superfluid density  $\hat{\rho}_s(T)$  in Eq.(26) so that it has  $\mathbf{r}$  dependence and satisfies  $\hat{\rho}_s(T;\mathbf{r}) = \int_V \hat{\rho}_s(T;\mathbf{r}) 2\pi r dr dz$  as

$$\hat{\rho}_s(T;\mathbf{r}) = \lim_{q \rightarrow 0} \frac{1}{q} \int_V \frac{q^2}{q} \hat{\mathbf{T}}(q;0;\mathbf{r}) r^2 d^3\mathbf{x} \quad ; \quad (31)$$

Let us consider the first approximation of the above quantities. We begin with

$$\langle J(\mathbf{x};t) \rangle = \langle \mathbf{G}^y \hat{\mathbf{J}}(\mathbf{x};t) S \mathbf{G}^y \rangle ; \quad (32)$$

where  $S = T \exp \left[ -i \int_0^{R_t} dt \hat{H}_{ex}(\mathbf{r};t^0) \right]$ . Using  $H_{ex}(\mathbf{r}) = \mathbf{v}_d(\mathbf{r}) \cdot \mathbf{J}(\mathbf{r})$ , the analytical continuation  $t \rightarrow i\tau$  is performed in the higher-order expansion terms in the right-hand side of Eq.(32) [17]. As the simplest nonlinear susceptibility for  $J$ , we consider the third-order term  $\langle \mathbf{v}_d \mathbf{v}_d \mathbf{v}_d \rangle^{(3)}$  with respect to  $H_{ex}$ , and extract a correction term to the linear susceptibility  $\langle \mathbf{v}_d \rangle^{(3)}$  from  $\langle \mathbf{v}_d \mathbf{v}_d \mathbf{v}_d \rangle^{(3)}$ .  $\langle \mathbf{v}_d \rangle^{(3)}$  is illustrated as a square in Fig.5 (a), in which we choose only one vertex for the coupling to  $\mathbf{v}_d(q)$  out of three vertices, and make the others couple to the coarse-grained external field  $\mathbf{v}_d(r)$ . The lowest-order dynamic response of  $I_z(\omega)$  is obtained through  $\langle \mathbf{v}_d \rangle^{(3)}$ . (From now, we express  $\langle \mathbf{v}_d \rangle^{(3)}$  by  $\langle \mathbf{v}_d \rangle^{(3)}(q;i)$ .)

Comparing Fig.4 (a) and Fig.5 (a), we find that  $p$  in the lower bubble of Fig.4 (a) splits into  $p$  and  $p_1$  in Fig.5 (a). Using Eq.(3), we obtain a formula corresponding to a square in Fig.5 (a)

$$\begin{aligned} {}^{(3)}(q; i!) = & \int \frac{1}{2} \int \frac{1}{2} \frac{1}{V^2} \frac{1}{p p_1} \left( p + \frac{q}{2} \right) \left( p_1 + \frac{q}{2} \right) \frac{p + p_1}{2} \frac{p + p_1}{2} + q \\ & G(i!_n + i!; p + q) G(i!_n; p) G(i!_m + i!; p_1 + q) G(i!_m; p_1); \end{aligned} \quad (33)$$

where  $[(p + p_1) = 2]$   $[(p + p_1) = 2 + q]$  comes from the coupling to the upper and lower  $v_d(r)$  in Fig.5 (a). In general, a loop with four vertices has three inner frequencies  $i!_n, i!_m$ , and  $i!_1$ . For the susceptibility like Fig.5 (a), however, the  $q; i!$  in  $(q; i!)$  enters at one of the four vertices and leaves at another, thus leaving only two frequencies  $i!_n, i!_m$  as internal ones in Eq.(33). The remaining  $\hat{H}_{ex}$  in  $\int_0^R d\hat{H}_{ex}$  corresponding to  $i!_1$  appears as  $\hat{H}_{ex}$  ( $= \int n_0 j_d(r) j$ ), since the macroscopic  $v_d(r)$  in  $\hat{H}_{ex}$  slowly varies with  $r$ .

(a) With decreasing temperature, the coherent wave functions gradually grow, and therefore the particle interchange owing to Bose statistics frequently occurs in  ${}^{(3)}$ . By applying Eq.(13)-like formula for the product of four currents, we obtain a perturbation expansion of  ${}^{(3)}$  with respect to the repulsive interaction  $H_I$ . Figure.5 (a) illustrates a square surrounded by a bubble in  $jg >$  (an analogue of Fig.4 (a)). The particle interchange at one of three vertices yields Fig.5 (b). Fig.5 (c) shows a horizontal and vertical extension of bubble chains.

(b) With decreasing temperature, particles stationary to a container get to play a dominant role. Comparing Fig.4 (c) and Fig.5 (b), we apply the argument above Eq.(15) to Eq.(33), knowing that  $p = 0$  and  $p = -q$  plays a dominant role in the sum over  $p$ . In the sum over  $p_1$  as well, the dominant process comes from  $p_1 = 0$  and  $p_1 = -q$ . At first sight, there seems to be four combinations in  $(p; p_1)$ . Owing to  $(p + p_1) = 2$  and  $(p + p_1) = 2 + q$  in Eq.(33), however, only  $(p; p_1) = (0; -q)$  and  $(-q; 0)$  are possible in Eq.(33). In Fig.5 (a), the coupling to  $v_d(q)$  is possible on the upper or lower vertices as well. Although this case has a different expression of  ${}^{(3)}(q; i!)$  from Eq.(33), the particle interchange and the dominance of  $p = 0$  or  $p = -q$  particles derive the same contribution to  ${}^{(3)}$ , hence giving the symmetry factor 2 to Eq.(33). Hence, one obtains for a square in Fig.5 (a)

$$\hat{\Lambda}^{(3)}(\mathbf{q}; 0; \mathbf{r}) = \frac{1}{V^2} \frac{q^2}{4} \int \frac{F(\mathbf{q})^2}{U F(\mathbf{q})^2} (\mathbf{r})^2 n_0(T); \quad (34)$$

The process like Fig.5 changes Eq.(34) as follows. Using Eq.(13)-like formula for the product of four currents, bubble chains in Fig.5(c) are extended to infinity. To derive the nonclassical behavior in Eq.(29), we pick up among these terms only terms which give a term proportional to  $q q = q^2$  at  $q \rightarrow 0$  limit, because other terms vanish in Eq.(29). Hence, we get

$$\hat{\Lambda}^{(3)}(\mathbf{q}; 0; \mathbf{r}) = \frac{q q}{2} \frac{q^2}{2} \frac{1}{V^2} \frac{1}{n^2} \frac{F(\mathbf{q})^2}{U F(\mathbf{q})^2} (\mathbf{r})^2 n_0(T); \quad (35)$$

Similarly to Eq.(18), the instability occurs in Eq.(35) when the condition of Eq.(20) is satisfied, because the denominator in the right-hand side of Eq.(35) gives  $q^4$ , and therefore the coefficient of  $q q$  diverges as  $q^2$  at  $q = 0$ . At  $T = T_{on}$ , the same procedure as that from Eq.(18) to (21) yields

$$\hat{\Lambda}^{(3)}(\mathbf{q}; 0; \mathbf{r}) = \frac{1}{V^2} \frac{2m}{U_{on}} \frac{1}{n^2} \tanh^2 \left[ \frac{m(T_{on})}{2} \right] (\mathbf{r})^2 n_0(T_{on}) \frac{q q}{q^2}; \quad (36)$$

and with the aid of Eq.(20)

$$\hat{\Lambda}^{(3)}(\mathbf{q}; 0; \mathbf{r}) = \frac{m n_0(T_{on})}{V^2} \frac{m (\mathbf{r})^2}{k_B T_{on}} \frac{1}{n^2 \sinh^2 \left( \frac{m(T_{on})}{2} \right)} \frac{q q}{q^2}; \quad (37)$$

Using  $\hat{\Lambda}_s(T) = m c(T) n_0(T)$  as in Eq.(23), we obtain

$$\hat{\Lambda}^{(3)}(\mathbf{q}; 0; \mathbf{r}) = m n_0(T_{on}) \frac{\hat{\Lambda}_s(T_{on})}{k_B T_{on}} \frac{m (\mathbf{r})^2}{q^2}; \quad (38)$$

Substituting Eq.(23) and (38) to Eq.(30) and using  $m n_0 = c^1(\hat{\Lambda}_s)$ , we get at  $T = T_{on}$

$$\rho_0(\mathbf{r}) = \frac{1}{4} \frac{\hat{\Lambda}_s(T)}{c(T)} \frac{1}{c(T)} \frac{\hat{\Lambda}_s(T)^3}{k_B T} \frac{m (\mathbf{r})^2}{5}; \quad (39)$$

Using Eq.(39), we obtain a velocity field  $\mathbf{v}_0(\mathbf{r}) = \rho_0(\mathbf{r}) \mathbf{r}$ , and a vorticity field

$$\text{rot} \mathbf{v}_0(\mathbf{r}) = \frac{2}{4} \frac{\hat{\Lambda}_s(T)}{c(T)} \frac{2}{c(T)} \frac{\hat{\Lambda}_s(T)^3}{k_B T} \frac{m (\mathbf{r})^2}{5} \mathbf{e}_z; \quad (40)$$

This form shows a little change from  $\text{rot} \mathbf{v} = 2 \mathbf{e}_z$  to  $\text{rot} \mathbf{v} = 0$ , that is, from a normal uid to a super uid. These results are summarized in the mechanical super uid density

$$\hat{\rho}_s(T; r) = \hat{\rho}_s(T)^4 \left[ 1 + \frac{1}{c(T)} \frac{\hat{\rho}_s(T)^{1/2}}{m} \frac{r^2}{k_B T} \right]^3 : \quad (41)$$

In a liquid helium 4,  $m = k_B = 2.13 \times 10^{-8} \text{ sec}^2/\text{cm}^2$ . Hence, the dependence of Eq.(41) is negligibly small. (Since the wall is not taken into account in the above formula, the position  $r$  in the right-hand side of Eq.(41) must be near the center of rotation.)

## V I. D I S C U S S I O N

### A . D i f f e r e n t i a l r o t a t i o n

In the normal phase, a liquid makes the rigid-body rotation satisfying  $\mathbf{v}_d(\mathbf{r}) = \boldsymbol{\omega} \times \mathbf{r}$ . In the super uid phase, a quantum vortex appears, and a liquid makes a peculiar rotation being independent of  $\boldsymbol{\omega}$  and satisfying  $\mathbf{v}(\mathbf{r}) = (h/m) \mathbf{e}_z \times \nabla \phi$  ( $\phi$  is an integer). At  $T < T < T_{\text{on}}$ , however, while a liquid is influenced by the rotation of a container, a region around the center of rotation slightly reduces its rotational velocity. Hence, its velocity field takes an intermediate form between these two limits. One can call it a kind of differential rotation [18]. As  $T \rightarrow T$ , the region with a slightly smaller vorticity appearing at the center of rotation enlarges toward the wall. To describe the growth of such a region, the effect of the wall must be taken into account as a boundary condition. At a given  $T$  in  $T < T < T_{\text{on}}$ , when the container slowly rotates, the region with a small rotational velocity occupies a relatively large portion of the container. With increasing  $\boldsymbol{\omega}$ , such a region will shrink to the center of rotation, and therefore the nonclassical  $I_z$  will approach the classical one.

In Sec.5, with  $r$  in  $\mathbf{v}_d(\mathbf{r}) = \boldsymbol{\omega} \times \mathbf{r}$  approaching the radius of container,  $\mathbf{v}_d(\mathbf{r})$  becomes a large external field, and more higher-order terms will contribute to  $I_z(\boldsymbol{\omega})$ . This will suppress super uidity, and  $\mathbf{v}_0(\mathbf{r}) = \mathbf{v}_d(\mathbf{r})$  with Eq.(39) will approach  $\mathbf{v}_d(\mathbf{r}) = \boldsymbol{\omega} \times \mathbf{r}$  of the rigid-body rotation. With increasing  $\boldsymbol{\omega}$  as well, one can expect a similar result. For the permutation symmetry to influence the behavior of the rapidly rotating system, the question is whether

a particle at  $r$  belonging to a wave function  $\psi$ , after one second, actually belongs to the same  $\psi$  at  $r + \Delta r$ . This probability depends not only on the size of the wave function but also on the frequency of appearance and disappearance of the Bose statistical coherence, a latter of which turns to the order parameter-order parameter correlation below  $T_c$ . When such calculations included,  $I_z(\omega)$  will be extrapolated to the classical  $I_z^{cl}$  as illustrated by a dotted line d in Fig.1.

At  $T < T_c$ , the nonclassical behavior discussed in this paper is masked by the quantum jump of  $L_z$  owing to the emergence of the quantum vortex. If the quantum vortex could be suppressed, one would see the hidden behavior of  $L_z(\omega)$ .

#### B. Shear viscosity at the vicinity of $T_c$

In Sec.1, we consider the decrease of viscosity just above  $T_c$  as a clue to understand the moment of inertia near  $T_c$ . As shown in Fig.2, the magnitude of this decrease reaches as much as 0.3 times of its maximum value at  $T = 2.8$  K, which is far larger than the estimated value of  $I_z = I_z^{cl}$  in Sec.4 using  $\rho = \rho_n$  in Ref. [5]. As long as we stick to the two-fluid model at the vicinity of  $T_c$ , we can find no clue to this problem. To explain this difference quantitatively, we must have a microscopic theory describing the influence of superfluidity on the coefficient of viscosity. For such a theory, one must apply the linear-response theory not to the mechanical, but to the thermal perturbation [19]. The formulation of the latter perturbation includes more subtle points than that of the former one owing to the thermal dissipation. The microscopic theory of the influence of superfluidity on  $\eta$  is a future problem.

Even if we have such a microscopic theory, however, one must notice that it is uncertain whether such a theory properly explain the observed large decrease of  $\eta$  occurring from 2.8 K to 2.17 K. The viscosity appears in the Navier-Stokes equation as  $\nabla \cdot \mathbf{v}$ , which has a form of  $\nabla \cdot (\text{rot}(\text{rot} \mathbf{v}))$  in an incompressible fluid. The decrease of the viscosity comes from either the decrease of  $\eta$  or that of  $\text{rot} \mathbf{v}$  [4]. The former is owing to the microscopic change of the system, whereas the latter comes from the macroscopic transformation of the velocity

field  $v(r)$  in a container [20]. Since the coherent wave function has not yet grown to a macroscopic size above  $T_c$ , its influence on the macroscopic  $v$  may be limited, and therefore it is natural to attribute the decrease of the viscosity just above  $T_c$  to the decrease of  $\rho_s$ . In

rot( $\rho v$ ), however, we have another possibility that the emergence of the intermediate-sized coherent wave function contributes to the decrease of  $\rho v$ . If it is true, this means that the microscopic mechanism of a liquid affects not only the coefficient  $\rho_s$ , but also the velocity field  $v(r)$  in the equation of fluid mechanics. In fluid mechanics, the velocity field  $v(r)$  is a solution of the equations with given mechanical or thermodynamical constants of a liquid. In the system like a liquid helium-4, one cannot clearly distinguish between the microscopic and macroscopic phenomena, and therefore this clear separation between the coefficient and solution of the equation is not obvious as in a classical liquid. Hence, one must make a different approach.

### C. Various manifestations of superfluidity

Superfluidity is a complex of phenomena, and therefore has some different definitions such as, (1) persistent current without friction, (2) the Hess-Fairbank effect, (3) quantized circulation, (4) almost no friction on moving objects in the system below the critical velocity, (5) peculiar collective excitations and (6) the Josephson effect. The conventional thermodynamical definition of superfluid density  $\rho_s(T)$  has been proved to be useful for describing various mechanical manifestations of superfluidity. The result of this paper implies that the superfluid density in the mechanical phenomena does not always agree with the thermodynamical  $\rho_s(T)$ , and that the interplay between Bose statistics and the repulsive interaction sometimes require us to define the mechanical superfluid density  $\hat{\rho}_s(T)$ . This  $\hat{\rho}_s(T)$  has a definition specific to each manifestation of superfluidity as  $\hat{\rho}_s(T)$  in Eq.(26) for the rotation. Hence, we must consider the existence or non-existence of  $\hat{\rho}_s(T)$  in each manifestation on a case-by-case basis. Here, we make a comment on three examples.

(A) The Meissner effect in the charged Bose system is a counterpart of the nonclassical

rotational behavior in the neutral Bose system [9] [10]. The phenomenon like the nonclassical  $I_z$  just above  $T_c$  occurs in the Meissner effect as well: With decreasing temperature, the charged Bose gas with short-range repulsion begins to exclude the magnetic field prior to the BEC [21]. This means that Bose statistics is essential for the Meissner effect, but the existence of the macroscopic condensate is not the necessary condition. The same form of the mechanical superfluid density  $\rho_s(T)$  is useful for the Meissner effect as well.

(B) The nonclassical rotational behavior above  $T_c$  will become more realistic in superfluidity of small systems. (1) The trapped atomic Bose gas falls into this category. The measurement of the angular momentum was performed [22], which is analogous to the experiment by Hess and Fairbank, and by Packard and Sanders in a bulk liquid helium-4. (2) Recently, a helium-4 droplet consisting of about  $10^4$  helium-4 atoms is found to show a sign of superfluidity. The infrared rotational spectrum of small molecules, such as oxygen carbon sulide, attached to the helium-4 droplet shows a signal indicating a significant change of its moment of inertia at  $T < T_c$ , which suggests the transition of surrounding helium-4 environment [23]. Although until now the experimental condition, such as temperature or the rotational velocity, cannot be freely controlled as in the bulk helium-4, it will open a new probability. If the same experiment as in Sec.4 could be made for a liquid helium-4 droplet, one would see a larger role of the intermediate-sized coherent wave function  $\psi_s(T_1) = \psi_s(T_c)$  in the rotational properties [8]. When the number of atoms in a droplet is too small, however, the transition will become obscure. Hence, there is probably an optimum system size for detecting the nonclassical rotational behavior just above  $T_c$ .

(C) Solid helium-4 has been termed a quantum crystal. Recently, an abrupt drop in the moment of inertia was found in the torsional oscillation measurements on solid helium-4 confined in a porous media [24] and on a bulk solid helium-4 [25]. This discovery leads us to reconsider the definition of superfluidity and that of solids [26]. The fundamental feature of crystals is their periodicity in density; that is, diagonal long-range order (DLRO). One has to face a serious question whether crystals remain stable while showing superfluidity that violates their periodicity. Phenomenologically, this discovery shares the following point with

the subject of this paper: The nonclassical decrease of the moment of inertia occurs even in the system in which the existence of the macroscopic Bose condensate is not expected. There is, however, the following difference. In a liquid helium 4 at the vicinity of  $T_\lambda$  in the normal phase, helium 4 atoms actually exist, and the size of their coherent wave function with zero momentum is a subject of the problem, whereas in a solid helium 4, the existence of a hypothetical moving boson, a zero-point vacancy, has not been firmly established, although it is normally assumed to exist. There are a number of problems to be clarified in a solid helium 4.



## REFERENCES

- [1] The shear viscosity of a liquid is inversely proportional to the rate of a process in which a hole in a liquid propagates from one point to another over the energy barriers. With decreasing temperature, this rate decreases, thus increasing the viscosity.
- [2] R D Taylor and J G Dash, *PhyRev*, 106, 398 (1957)
- [3] The variational theory at the vicinity of  $T_c$ , which assumes the expandibility of the thermodynamic potential in powers of the small order parameter, belongs to this category.
- [4] F London *Super uid*, (John Wiley and Sons, New York, 1954) Vol2, 141.
- [5] G B Hess and W M Fairbank, *PhyRev*, 19, 216 (1967)
- [6] As a text, R J Donnelly, *Quantized Vortices in Helium II*, (Cambridge, 1991)
- [7] R E Packard and T M Sanders, *PhyRev*, 6, 799 (1972)
- [8] In the equation of states  $N/V = g_{3/2}(e^{-\beta\epsilon}) + V^{-1} e^{-\beta\epsilon} = (1 - e^{-\beta\epsilon})^{-1}$  where  $g_a(x) = \sum_n x^n / n^a$ ,  $V^{-1} e^{-\beta\epsilon} = (1 - e^{-\beta\epsilon})^{-1}$  has a finite value at  $V \rightarrow \infty$  limit only when  $e^{-\beta\epsilon} = (1 - e^{-\beta\epsilon})^{-1}$  diverges. Hence, this limit decomposes all states into only two classes, the condensate and the whole of other states, and therefore each of other states loses its characteristics.
- [9] As a review, P Nozieres, in *Quantum Fluids* (ed by D E Brewer), 1 (North Holland, Amsterdam, 1966).
- [10] As a review, G Baym, in *Mathematical methods in Solid State and Super uid Theory* (ed by R C Clark and G H Derrick), 121 (O liver and Boyd, Edinburgh, 1969)
- [11] This treatment enables us to derive the super uid density in any complicated approximation of the susceptibility.
- [12] R P Feynman, in *Progress in Low Temp Phys.* 1, (ed C J Gorter), 17 (North-Holland, Amsterdam, 1955).

- [13] It is possible that more complex diagrams than the bubble in  $JG > m$  may participate in the particle exchange with the tensor  $JJ$  in Fig.4(a). While it is difficult to estimate an infinite sum of these diagrams, it adds only a small correction to the whole feature of the phenomenon.
- [14] In an attractive Bose gas ( $U < 0$ ), the instability condition leading to a liquid state is recently found as  $(T) = \frac{p}{U k_B T}$  in S K oh, *PhyRev,E*,72, 016104 (2005). It is suggestive that, in a response to the external perturbation, a similar-looking instability condition  $(T) (U) = \frac{p}{U k_B T}$  appears in a different context of the repulsive Bose system ( $U > 0$ ).
- [15] T Matsubara, *Prog.Theo.Phys.*6, 714 (1951).
- [16] R P Feynman, *PhysRev.* 90, 1116 (1953), *ibid* 91, 1291 (1953).
- [17] The analytic continuation between the real-time susceptibility and the imaginary-time one was originated by Abrikosov, Gorkov and Dzyaloshinskii. This procedure was extended to the higher-order susceptibility in the interaction representation by V.V Slezov in *Fiz.Tverd.tela*,5, 2958 (1963) [*Sov Phys-Solid State*,5, 2166 (1963)]
- [18] In contrast with the differential rotation of rotating stars or galaxies in astrophysics, a central region does not follow the rigid-body rotation.
- [19] L P Kadano and P.C Martin, *Ann Phys.* 24, 419 (1963).
- [20] At  $T < T_c$ , the temperature dependence of the shear viscosity strongly depends on the experimental methods, such as (1) a Poiseuille flow method (a lower horizontal line at  $T < T_c$  in Fig.2), (2) a rotation viscometer method and (3) an oscillating disc viscometer method (an upper curve at  $T < T_c$ ). This fact suggests that the shear viscosity at  $T < T_c$  is strongly dependent on the change of rotv.
- [21] S K oh, *PhyRev B*, 68, 144502 (2003).

- [22] F Chevy, K W Madison and J Dalibard, *PhysRev.Lett.* 85, 2223 (2000).
- [23] S Grebenev, J P Toennies and A F Vilesov, *Science* 279, 2083 (1998).
- [24] E Kim and M H W Chan, *Nature*. 427, 225 (2004).
- [25] E Kim and M H W Chan, *Science*. 305, 1941 (2004).
- [26] A J Leggett, *PhysRev.Lett* 25, 1543 (1970).

## FIGURES

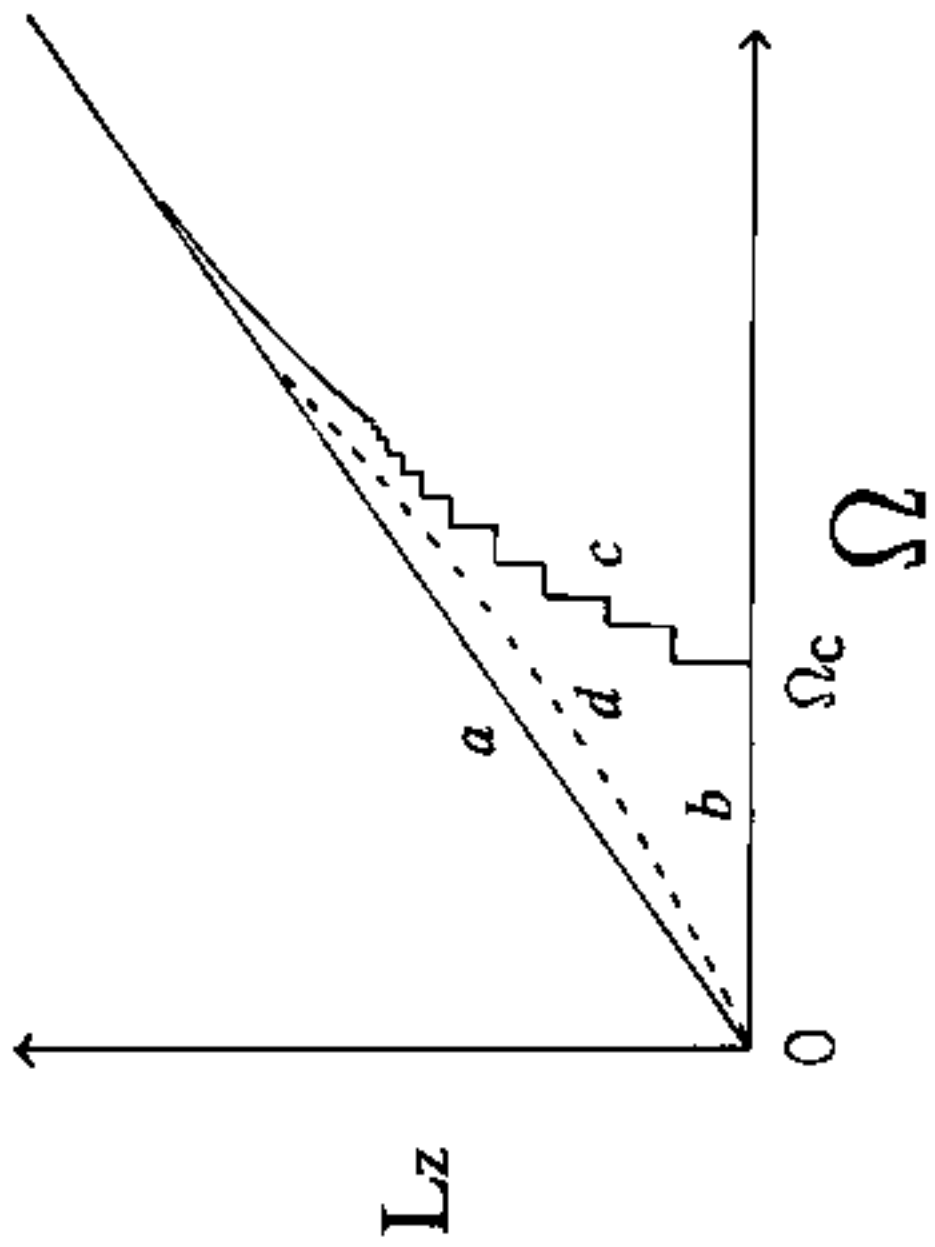
FIG .1. The dependence of the angular momentum  $L_z$ . A solid straight line a is  $L_z = I_z^{\text{cl}}$  at  $T = T_c$ , and a horizontal line b and a series of steps c is  $L_z(T)$  at  $T < T_c$ . A dotted curve d is a subject of this paper.

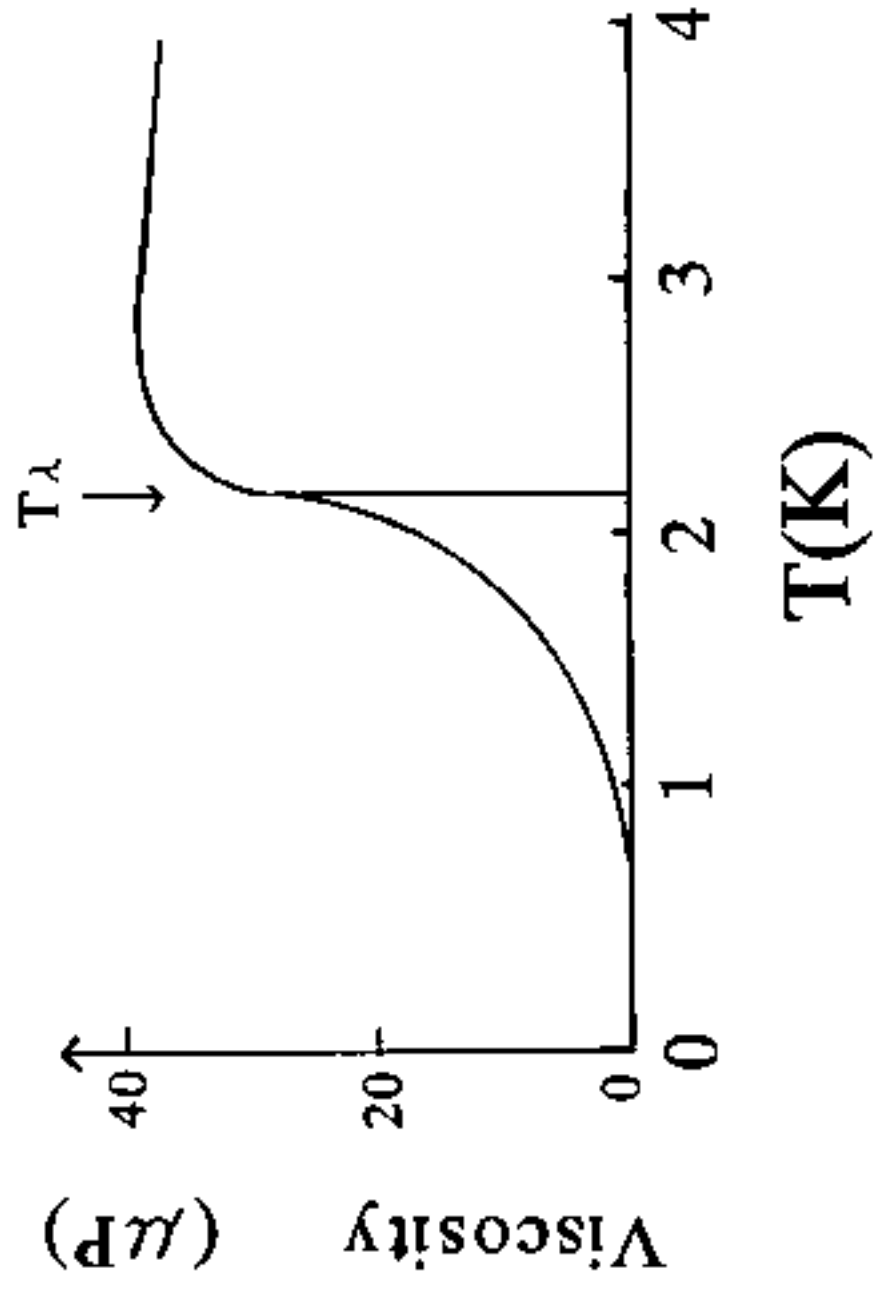
FIG .2. The temperature dependence of the shear viscosity of a liquid helium  $^4\text{He}$ . (At  $T < T_c$ , the data depend on the experimental method.)

FIG .3. Schematic pictures of a part of the rotating bosons in a cylindrical container. White circles represent a initial distribution of particles. The rotation by long arrows moves white circles on a solid-line radius to black circles. (a) At  $T < T_c$ , the permutation symmetry holds over the entire liquid. (b) Just above  $T_c$ , it holds only within limited areas enclosed by a dotted lines.

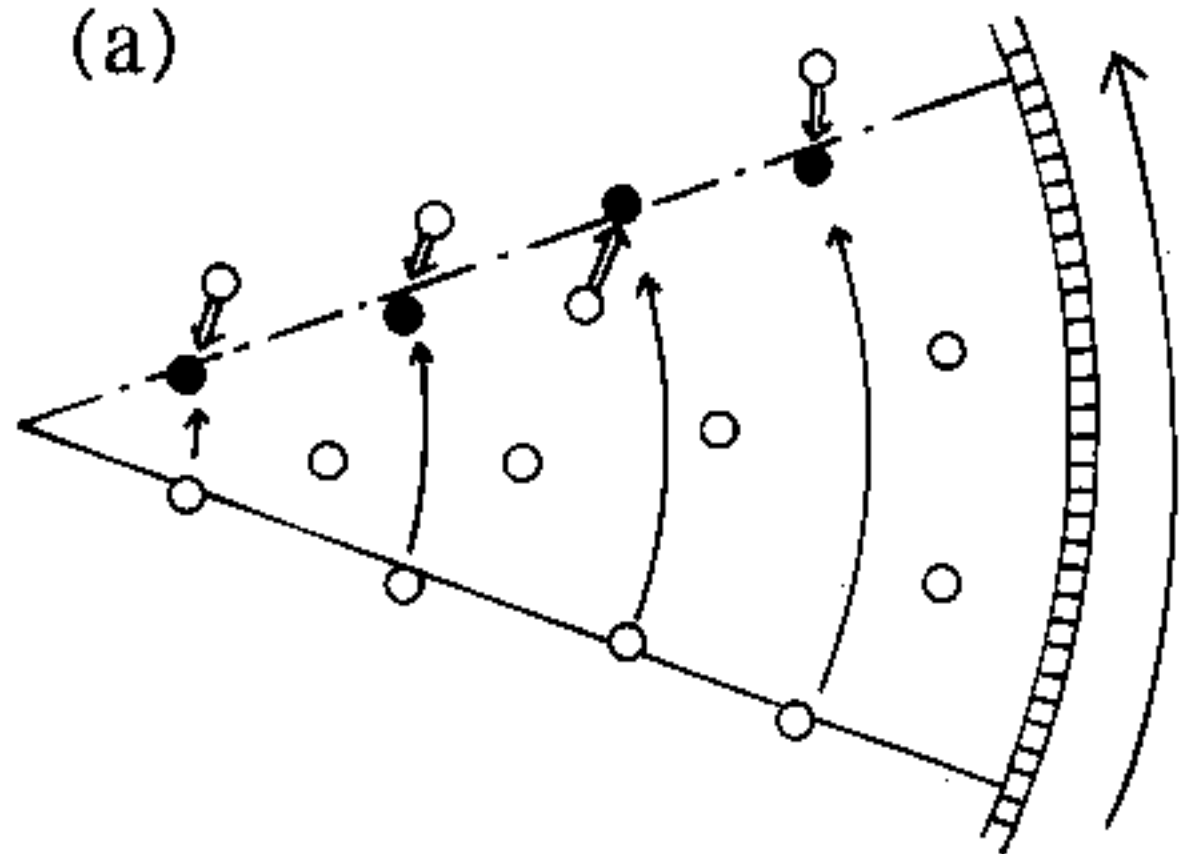
FIG .4. (a) The first-order Feynman diagram of a current-current response tensor  $J J$  (a lower bubble), and an excitation owing to the repulsive interaction  $U$  (an upper bubble with a dotted line). The black and white small circle represents a vector and a scalar vertex, respectively. The exchange of particle lines between the excitation and the response tensor yields (b). Similarly, the interchange of particle lines in a deformed square yields (c).

FIG .5. (a) The third-order Feynman diagram of the current-current response tensor accompanied by the bubble excitation. (The definition of symbols is same as in Fig.4.) The exchange of particle at one vertex yields (b). Similar exchanges at the other vertices yield (c).

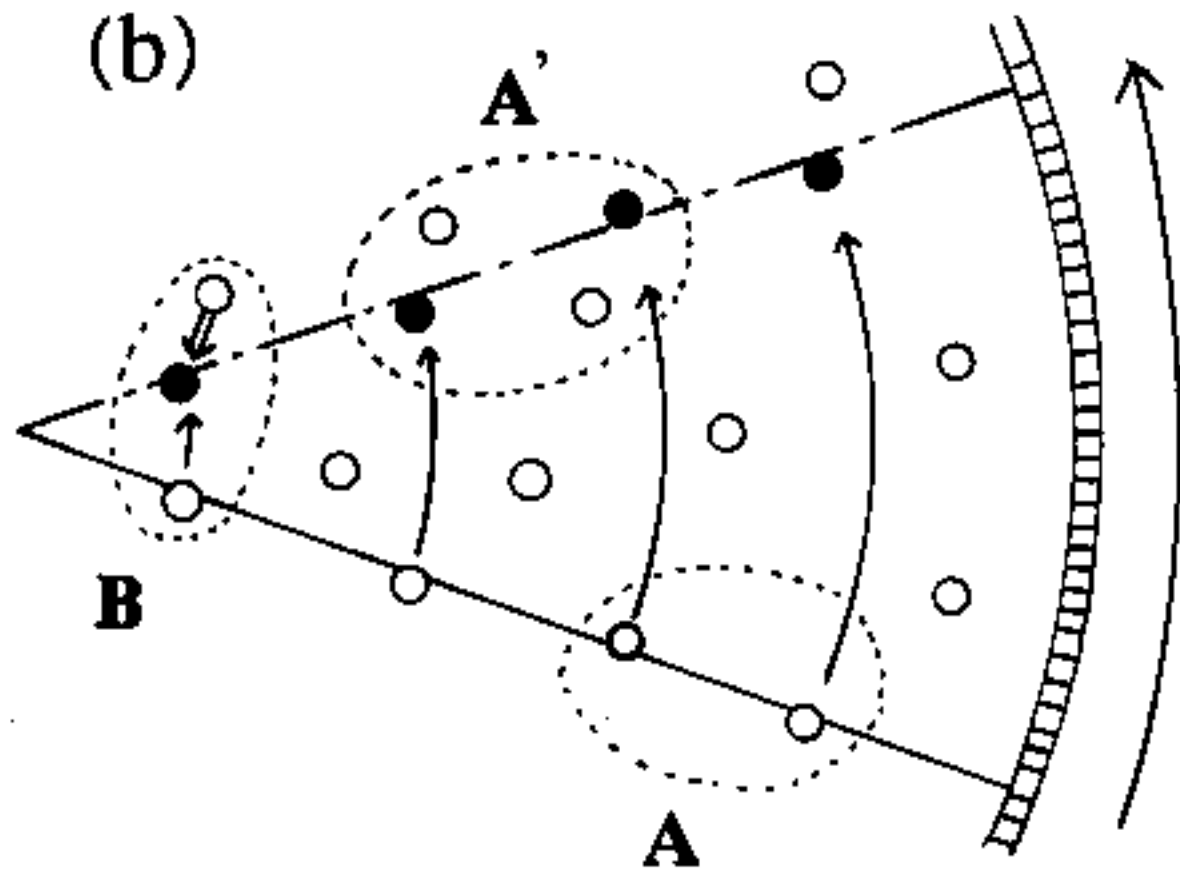


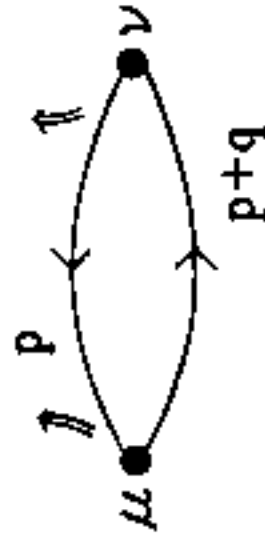
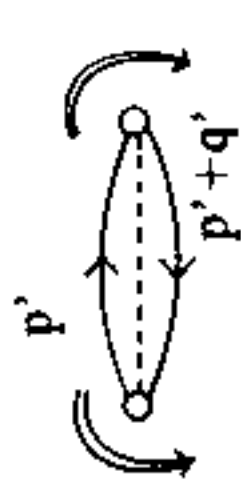


(a)

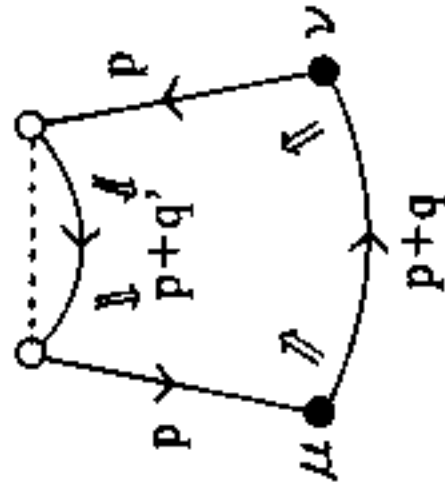


(b)

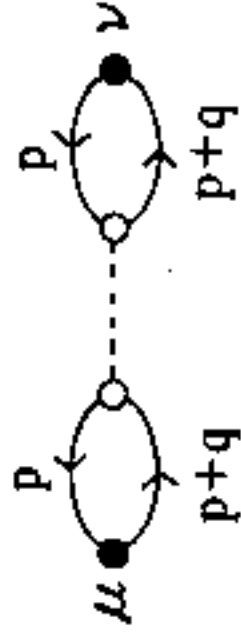




(a)



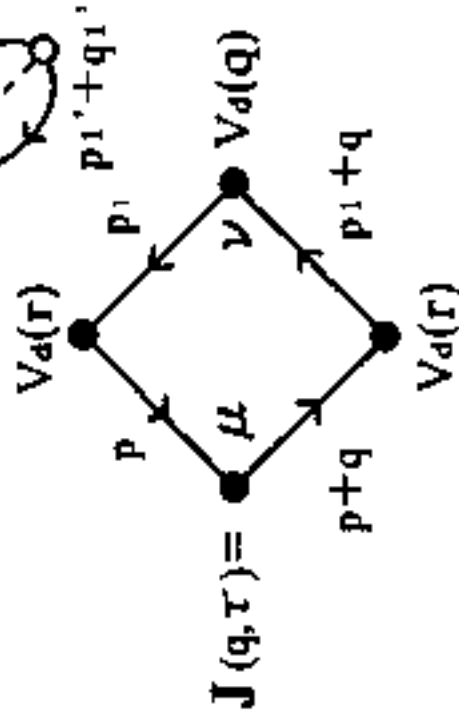
(b)



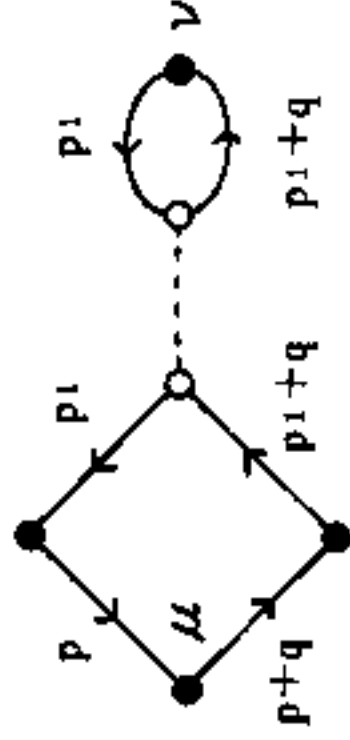
(c)



(a)



(b)



(c)

